

# MASP: Scalable GNN-based Planning for Multi-Agent Navigation

Xinyi Yang<sup>1\*</sup>, Xinting Yang<sup>1\*</sup>, Chao Yu<sup>1✉</sup>, Jiayu Chen<sup>1</sup>, Huazhong Yang<sup>1</sup> and Yu Wang<sup>1✉</sup>

**Abstract**—We investigate the problem of decentralized multi-agent navigation tasks, where multiple agents need to reach initially unassigned targets in a limited time. Classical planning-based methods suffer from expensive computation overhead at each step and offer limited expressiveness for complex cooperation strategies. In contrast, reinforcement learning (RL) has recently become a popular paradigm for addressing this issue. However, RL struggles with low data efficiency and cooperation when directly exploring (nearly) optimal policies in the large search space, especially with an increased agent number (e.g., 10+ agents) or in complex environments (e.g., 3D simulators). In this paper, we propose *Multi-Agent Scalable GNN-based Planner* (MASP), a goal-conditioned hierarchical planner for navigation tasks with a substantial number of agents. MASP adopts a hierarchical framework to divide a large search space into multiple smaller spaces, thereby reducing the space complexity and accelerating training convergence. We also leverage graph neural networks (GNN) to model the interaction between agents and goals, improving goal achievement. Besides, to enhance generalization capabilities in scenarios with unseen team sizes, we divide agents into multiple groups, each with a previously trained number of agents. The results demonstrate that MASP outperforms classical planning-based competitors and RL baselines, achieving a nearly 100% success rate with minimal training data in both multi-agent particle environments (MPE) with 50 agents and a quadrotor 3-dimensional environment (OmniDrones) with 20 agents. Furthermore, the learned policy showcases zero-shot generalization across unseen team sizes.

## I. INTRODUCTION

Navigation is an important task for intelligent embodied agents, widely applied in various domains, including autonomous driving [1], [2], logistics and transportation [3], [4], and disaster rescue [5], [6]. In this paper, we consider a decentralized multi-agent navigation problem where multiple agents make decisions independently and simultaneously navigate towards a set of initially unassigned targets, which is more challenging in cooperation.

Planning-based solutions have been extensively employed in multi-agent navigation tasks [7], [8]. They offer the advantage of minimal training and adaptability to varying agent numbers. However, these methods often exhibit limited capabilities in coordination strategies, demanding intricate

hyper-parameter tuning for each specific scenario. Moreover, they can be time-consuming due to frequent re-planning at each decision step. Conversely, reinforcement learning (RL) has attracted significant attention for its remarkable expressiveness in multi-agent navigation tasks [9], [10], [11]. RL-based methods involve the direct end-to-end learning of neural policies by interacting with a simulated environment. Compared to planning-based solutions, RL-based methods offer strong representation capabilities for complex strategies and negligible inference overhead once the policies are well-trained.

In RL [12], [13], the prevailing approach to finding near-optimal solutions is to directly train a policy that produces environmental actions for agents. However, directly learning strategies from large search spaces results in low data efficiency and limited cooperation, which is more severe with increased agent numbers or environmental complexity. Therefore, existing methods [14], [15] mainly focus on navigation tasks in simple scenarios with only a few agents.

To solve these challenges in navigation tasks with a substantial number of agents, we adopt a hierarchical framework to divide a large search space into multiple smaller spaces, resulting in reduced space complexity and improved data efficiency. For improved goal achievement and cooperation, we leverage graph neural networks (GNN) to capture the interaction between agents and goals. Besides, to enhance generalization capabilities in scenarios with unseen team sizes, we divide the agents into multiple groups, each with a fixed number of agents during both training and evaluation. Therefore, we can always assume that each agent is in the previously seen group. We call this overall solution, *Multi-Agent Scalable GNN-based Planner* (MASP).

MASP comprises two components: a Multi-Goal Matcher (MGM) for goal assignment and a Coordinated Action Executor (CAE) for goal achievement. In MGM, each agent utilizes graph matching to determine the probability distribution of goals, subsequently selecting the most appropriate goal at each global step. In CAE, we develop a Graph Merger to perceive inter-agent relationships and a Goal Encoder to capture the correlation between the agent and its designated goal, thereby promoting cooperation.

We compare MASP against planning-based methods and RL-based variants in multi-agent particle environments (MPE) [16] and a 3-dimensional (3-D) quadrotor environment (OmniDrones) [17]. Empirical results demonstrate that MASP outperforms RL baselines, achieving a nearly 100% success rate with minimal training data. In evaluation, MASP attains at least 18.26% fewer steps in MPE with 50 agents and 7.06% fewer steps in Omnidrones with 20 agents. Moreover, MASP exhibits zero-shot generalization in scenarios with unseen

\* Equal Contribution

✉ Corresponding Authors

<sup>1</sup>Department of Electronic Engineering, Tsinghua University, Beijing, 100084, China. yang-xy20@mails.tsinghua.edu.cn

We acknowledge Botian Xu for providing the guidance on OmniDrones.

This research was supported by National Natural Science Foundation of China (No.62325405, U19B2019, M-0248), Tsinghua University Initiative Scientific Research Program, Tsinghua-Meituan Joint Institute for Digital Life, Beijing National Research Center for Information Science, Technology (BNRist) and Beijing Innovation Center for Future Chips.

More information can be found at <https://sites.google.com/view/masp-ral>.

team sizes, achieving at least 11.99% fewer steps in MPE. In OmniDrones, MASP has an average 92.5% success rate, while other baselines fail to complete the task in any episode.

## II. RELATED WORK

### A. Multi-agent Navigation

Reinforcement learning is widely adopted in navigation tasks for its adaptive and effective strategies [18], [19], [20]. However, multi-agent navigation tasks [9], [10], [21] bring challenges due to their large search space, resulting in low data efficiency and cooperation, especially in scenarios with a substantial number of agents. DARLIN [22] restricts the agent interactions to one-hop neighborhoods to break the curse of dimensionality. However, DARLIN overlooks interactions among all agents, increasing the risk of collisions in complex environments. MAGE-X [10] introduces a hierarchical approach that centrally allocates target goals to the agents at the beginning of the episode and then utilizes GNN to construct a subgraph for each agent. Nonetheless, this method is under a centralized paradigm, which is difficult to adapt to different team sizes. In this paper, we propose a decentralized GNN-based hierarchical framework for navigation tasks in MPE and a complex quadrotor 3-D simulator, Omnidrones, with unseen and large numbers of agents.

### B. Goal-conditioned HRL

Goal-conditioned hierarchical reinforcement learning (HRL) has been shown to be effective in various tasks [23], [24], [25]. In general, goal-conditioned HRL comprises two policies: an upper policy selects high-level subgoals at each global timestep, and a lower policy predicts environmental actions to achieve these subgoals. However, a lack of interaction between policies at different levels may raise a challenge, where changes in the low-level policy can lead to non-stationarity in the high-level policy. [26] solves this problem by sending the policy representation of the low-level policy to the high-level policy. Moreover, existing approaches with explicit subgoals [24], [27] heavily rely on manually pre-defined subgoals. Director [23] selects implicit subgoals in the latent space, thereby eliminating the need for complex manual design. However, these methods are less suitable for scenarios with multiple initially unassigned targets, as they struggle to establish connections between subgoals and final targets. In this work, we develop a goal assignment module as the high-level policy, where multiple goals are directly assigned to agents at each global decision-making step.

### C. GNN

Graph neural networks [28] excel at modeling complex relationships between diverse entities. They have been widely used in various applications, including social networks [29] and molecular structure [30]. In multi-agent systems, GNN is utilized to capture the interactions among agents. G2ANet [31] constructs a fully connected graph and employs a two-stage attention network to capture interactions between two agents. [32] proposes a GNN-based model that combines egocentric views with allocentric views. This

approach jointly predicts the trajectories of all agents and improves the inference speed. In this paper, we utilize GNN to capture the correlation between agents and goals for enhanced goal achievement and cooperation.

## III. TASK SETUP

We consider multi-agent navigation tasks with initially unassigned goals, which is more challenging for cooperation. Each episode starts with a random initialization of  $N$  agents and  $N$  landmarks. Agents are not assigned goals initially and are required to make global decisions every 3 environmental steps for goal assignment. We assume that the agents have access to the locations of other agents and target goals. When the agents reach all the landmarks, the task is 100% successful.

## IV. METHODOLOGY

### A. Overview

To solve the issues of low sample efficiency in navigation tasks with substantial numbers of agents, we adopt a hierarchical framework that partitions the large search space into multiple smaller spaces, resulting in reduced space complexity and faster training convergence. Moreover, we utilize GNN to capture the correlation among agents for enhanced cooperation. As depicted in Fig. 1, we introduce this overall framework, *Multi-Agent Scalable GNN-based Planner*, which consists of two components: a Multi-Goal Matcher for goal assignment and a Coordinated Action Executor for goal achievement.

Take agent  $k$  as an example. We first construct two types of graphs, one containing the position information of agents and the other including that of target goals. MGM then takes in these two graphs for graph matching and assigns agent  $k$  the most appropriate target based on the matching score at each global step. Receiving the designated goal, agent  $k$  leverages the Goal Encoder in CAE to extract the relationship between itself and the goal. Meanwhile, to improve the generalization in the scenarios with unseen agent numbers, we divide all agents into several groups, and the Graph Merger in CAE transforms the groups into graphs, each with a fixed number of nodes (i.e., agents) for both training and evaluation. The Graph Merger then perceives the correlation between agents and yields the updated feature of agent  $k$  across all graphs. The updated feature of agent  $k$ , together with the extracted embedding from the Goal Encoder, is sent into the State Extractor to endow the team representation with strong goal guidance. Finally, agent  $k$  takes the environmental action from the Action Generator to navigate towards the goal.

We train MGM and CAE simultaneously by using multi-agent proximal policy optimization (MAPPO) [12], a multi-agent variant of proximal policy optimization (PPO) [33].

### B. Multi-Goal Matcher

Goal assignment is a long-studied maximum matching problem, which is known to be NP-hard [34], [35]. The Hungarian algorithm [36] is a classical combinatorial optimization algorithm that solves the assignment problem. However, it centrally calculates the total distance cost and yields matching pairs with minimum cost, which is unsuitable

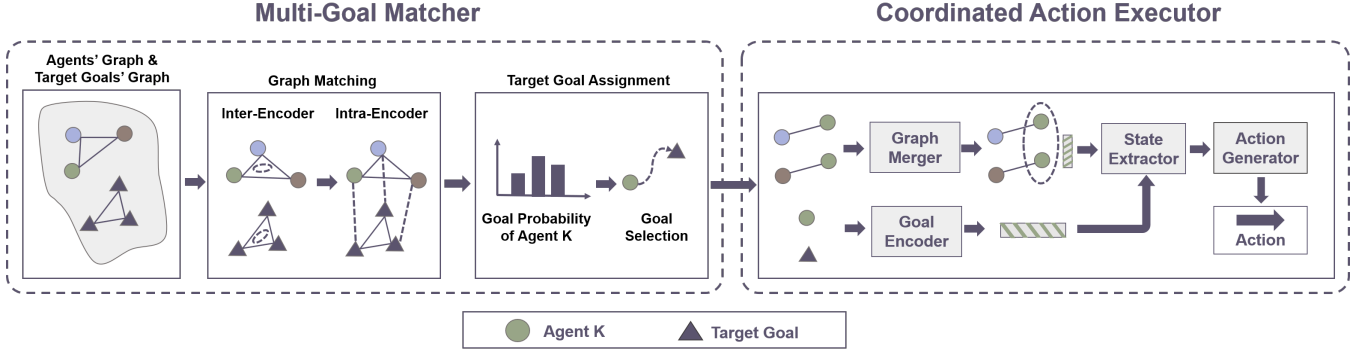


Fig. 1: Overview of *Multi-Agent Scalable GNN-based Planner*. Here, we take Agent  $k$  as an example.

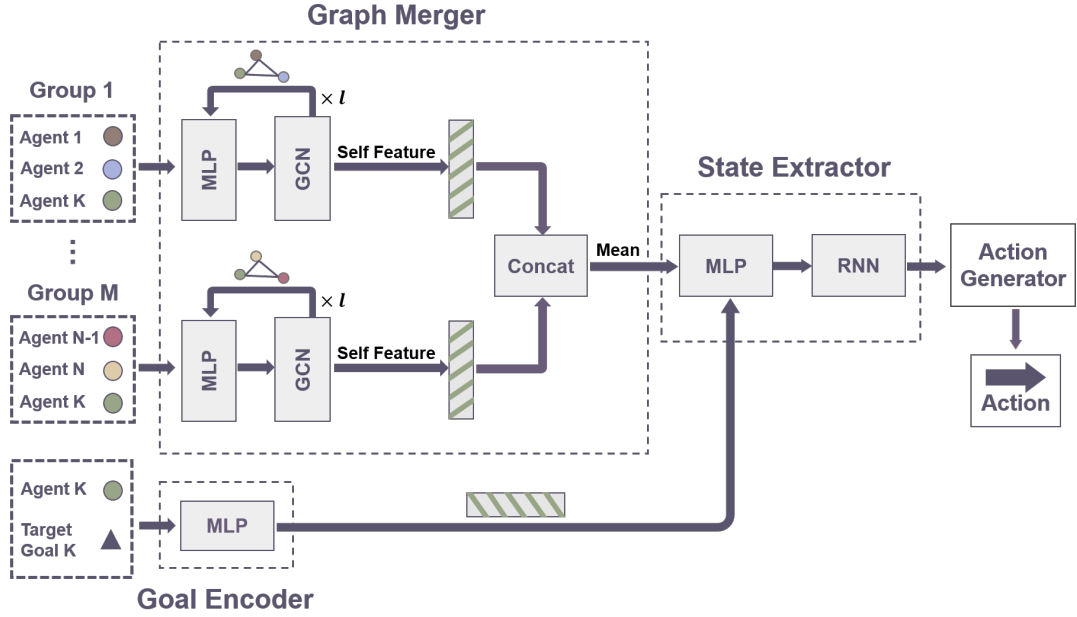


Fig. 2: Workflow of *Coordinated Action Executor*, including a Graph Merger to perceive agent interaction, a Goal Encoder to embed goal guidance, a State Extractor for state representation learning, and an Action Generator to produce environmental actions. We take Agent  $k$  as an example.

for our decentralized setting. To solve this problem, we introduce a decentralized RL-based Matcher, the Multi-Goal Matcher, to assign an appropriate target goal to each agent at each global step. More concretely, agent  $k$  first receives two types of fully connected graphs, one containing the position information of agents in nodes and the other containing that of target goals in nodes. Afterward, we leverage self-attention [37] in the Inter-Encoder for each graph to perceive the spatial relationship between the agents/the target goals and update the node features. To calculate the attention weight between agent  $k$  and the target goals, we further employ cross-attention [37] in the Intra-Encoder to generate the probability distribution of the target goals. Finally, agent  $k$  chooses the most appropriate goal to achieve independently.

The design of the reward function for MGM draws inspiration from the Hungarian algorithm. The reward for agent  $k$ ,  $R_m^k$ , is formulated as follows:

$$R_m^k = \begin{cases} 0, & G_m^k == G_h^k; \\ -(1 + \frac{N_{repeat}}{N}), & G_m^k \neq G_h^k \text{ and } G_m^k \in G_m^{-k}; \\ -(1 - \frac{C_h}{C_m}), & G_m^k \neq G_h^k \text{ and } G_m^k \notin G_m^{-k}. \end{cases}$$

Here  $G_m^k$  represents the predicted goal from MGM for agent  $k$ , and  $G_h^k$  denotes the goal assigned by the Hungarian algorithm. Additionally,  $C_m$  denotes the total distance from the predicted goals to the agents, while  $C_h$  is the total distance from the Hungarian assigned goals to the agents.  $N$  denotes the total number of agents, and  $N_{repeat}$  signifies the number of other agents whose predicted goal is the same as the predicted goal of agent  $k$ .

### C. Coordinated Action Executor

We introduce the Coordinated Action Executor to encourage agents cooperatively to reach the assigned goals from MGM. The workflow of CAE is illustrated in Fig. 2. To

enhance the generalization capability in scenarios with an unseen number of agents, we divide the agents into several groups, each with a fixed number of agents (i.e., 3 in our work) during both training and evaluation. Therefore, we can always assume that each agent is in the previously seen group. The number of groups depends on the agent count, and we may assign the same agent to more than one group to ensure that each group has the same fixed number of agents. Besides, agent  $k$  must be contained in each group so that we can update the node feature of agent  $k$  by perceiving the relationships between agent  $k$  and other agents in each group.

We first encode the state of the agents and transform each group into a graph. The Graph Merger then perceives the relationships between agent  $k$  and other agents in each graph and yields the updated feature of agent  $k$  across the graphs. Meanwhile, the Goal Encoder extracts the correlation between agent  $k$  and its designated goal, which is subsequently fed into the State Extractor along with the updated feature of agent  $k$ . Finally, the Action Generator produces the environmental action for the agent  $k$  to navigate towards the goal.

The reward,  $R_t^k$ , for agent  $k$  in the CAE is a linear combination of the complete bonus,  $R_b$ , the distance penalty,  $R_d$ , and the collision penalty,  $R_c$ :

$$R_t^k = \alpha R_b^k + \beta R_d^k + \gamma R_c^k,$$

where  $\alpha$ ,  $\beta$  and  $\gamma$  are the coefficients of  $R_b^k$ ,  $R_d^k$  and  $R_c^k$ , respectively.

1) *Graph Merger*: The Graph Merger models the interaction between agents via graph convolutional networks (GCN). We first obtain the groups of agents and apply an MLP layer to encode the state of the agents. Afterward, the Graph Merger utilizes GCN to generate a fully connected graph for each group, where the nodes contain the state of the agents. We consider the above process as a block, and the Graph Merger consists of  $l$  blocks (i.e., 2 in our work). Subsequently, we concatenate the node feature of agent  $k$  from all the graphs and perform a mean operation on the combined feature, yielding the updated feature for agent  $k$ .

2) *Goal Encoder and State Extractor*: To endow the agent  $k$  with strong goal guidance, the Goal Encoder is designed to extract the goal representation by considering the target goal's position and the agent's state. Receiving the relationship between the agent and its target goal, as well as the updated feature of agent  $k$  from the Graph Merger, the State Extractor leverages an MLP layer and recurrent neural networks (RNN) to perceive the historical and current state representations.

## V. EXPERIMENTS

### A. Testbeds

To evaluate the effectiveness of our approach in the large search space, we opt for two experimental environments: MPE [16] and OmniDrones [17], both involving a substantial number of agents.

1) *MPE*: MPE is a classical 2-dimensional environment, as shown in Fig. 3(a). The collision between agents results in a disruptive bounce-off effect, adversely impacting navigation efficiency. The available discrete actions of the agents include

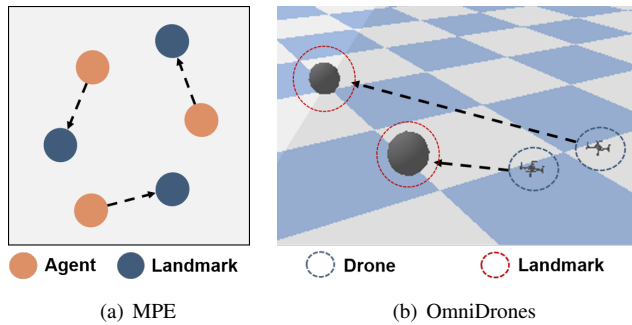


Fig. 3: The chosen testbeds.

*Up*, *Down*, *Left*, and *Right*. The experiment is conducted on scenarios with  $N \in \{5, 20, 50\}$  agents, each with randomized spawn locations for both agents and landmarks on the maps sized at  $4m^2$ ,  $64m^2$ , and  $400 m^2$ , respectively. Additionally, the horizons of the environmental steps for  $N = 5, 20$ , and  $50$  are set to 18, 45, and 90, respectively.

2) *OmniDrones*: As displayed in Fig. 3(b), we further conduct experiments in Omnidrones, which is an efficient and flexible 3-D simulator designed for drone control, to showcase the performance of MASP in the complex search space. The continuous action space of each drone is the throttle for each motor. Collisions between drones directly lead to crashes and task failures, heightening the challenge of completing the task. We conduct experiments with  $N \in \{5, 20\}$  drones, where the spawn locations for both drones and landmarks are randomly distributed on the maps sized at  $36m^2$  and  $256m^2$ , respectively. Besides, the horizons of the environmental steps for  $N = 5$  and  $20$  are set to 300 and 500, respectively.

### B. Implementation Details

Each RL training is performed over 3 random seeds for a fair comparison. Each evaluation score is expressed in the format of "mean (standard deviation)", which is averaged over a total of 300 testing episodes, i.e., 100 episodes per random seed. Our experimental platform involves a 256-core CPU, 256GB RAM, and eight NVIDIA GeForce RTX 3090Ti with 24GB VRAM.

### C. Evaluation Metrics

We consider 2 statistical metrics to capture different characteristics of a particular navigation strategy.

- **Success Rate (SR)**: This metric denotes the ratio of the number of landmarks reached by the agents to the total number of landmarks.
- **Steps**: This metric represents the timesteps required to achieve a target *Success Rate* within an episode.

### D. Baselines

We challenge MASP against three representative planning-based approaches (ORCA, RRT, Voronoi) and three prominent RL-based solutions (MAPPO, DARL1N, MAGE-X). Note that when applying the planning-based approaches to navigation, we utilize a greedy algorithm for decentralized goal assignment, where each agent is sequentially allocated to the nearest goal without duplication.

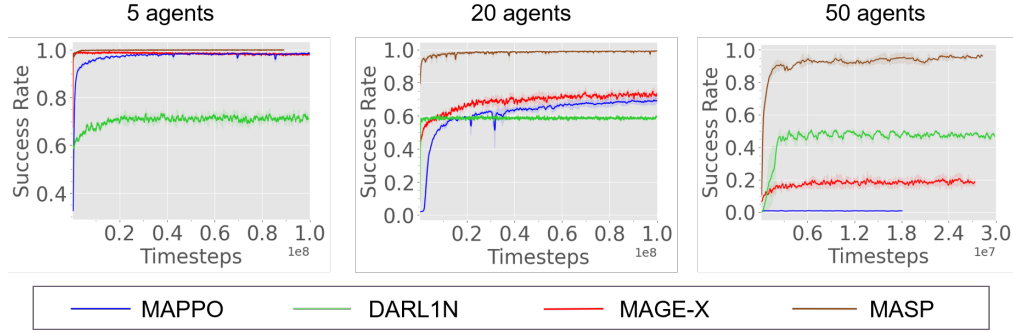


Fig. 4: Comparison between MASP and other baselines in MPE with  $N = 5, 20, 50$ .

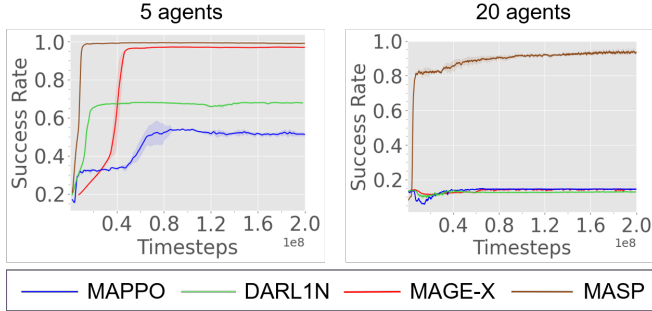


Fig. 5: Comparison between MASP and other baselines in Omnidrones with  $N = 5, 20$ .

- **ORCA** [38]: ORCA is an obstacle avoidance algorithm that excels in multi-agent scenarios. It predicts the movements of surrounding obstacles and other agents, and then plans the speed of collision avoidance.
- **RRT** [8]: RRT is a sample-based path planning algorithm that omits the consideration of complex kinematic constraints. It is suitable for solving path-planning problems under high-dimensional spaces and complex constraints.
- **Voronoi** [39]: A Voronoi diagram comprises a set of continuous polygons where a vertical bisector of lines connects two adjacent points. By partitioning the map into Voronoi units, a path can be planned from the starting point to the destination at a safe distance.
- **MAPPO** [12]: MAPPO is the first and the most straightforward implementation of PPO in the multi-agent setting. Each agent is equipped with a policy with a shared set of parameters, and we update this shared policy based on the aggregated trajectories of all agents. We additionally replace the MLP backbone with the attention mechanism to enhance the model’s capabilities.
- **DARL1N** [22]: DARL1N is a distributed method for large-scale agent scenarios. It breaks the curse of dimensionality in the policy by restricting the agent interactions to one-hop neighborhoods.
- **MAGE-X** [10]: This is a hierarchical approach to multi-agent navigation tasks. It first centrally allocates target goals to the agents at the beginning of the episode and then utilizes GNN to construct a subgraph only with important neighbors for higher cooperation.

## E. Main Results

### 1) Training with a Fixed Team Size:

**MPE:** We present the training curves in Fig. 4 and the evaluation performance in Tab. I. The results indicate that MASP performs the best with the least training data, where the advantage in *Steps* and *Success Rate* is more obvious as the number of agents increases. Compared to the RL baselines, especially in scenarios with 50 agents, MASP achieves a *Success Rate* of nearly 100%, while others fail to complete the task in any episode. This indicates that the GNN-based hierarchical framework in MASP has the capability to effectively handle the problem of large search spaces and enhance training efficiency. Among all RL baselines, DARL1N exhibits the best results in  $N = 50$  with a 49% *Success Rate*, while it shows the worst performance in  $N = 5$ . This implies that when the scenario only has a few agents, perceiving one-hop neighborhoods may lead to a situation where none of the agents is in the one-hop, thereby influencing the agents’ decisions. MAGE-X has a 23% *Success Rate* in  $N = 50$ , suggesting that the MLP-based goal assignment module encounters challenges in designating targets that can prevent collisions or tromboning for a large number of agents. MAPPO exhibits the worst performance with only 0.01% *Success Rate* in  $N = 50$ , implying that it is difficult for agents to directly extract the correlation among agents based on the given information and identify which goals they should reach.

Regarding planning-based competitors, Voronoi shows the best performance. Compared to MASP, Voronoi has an on-par *Success Rate* and 18.26% more *Steps* in  $N = 50$ . This suggests that Voronoi partitions set agents apart to reduce collisions and enable agents to reach the targets more quickly. As the number of agents increases, ORCA and RRT perform worse with around  $2\times$  more *Steps* than MASP in  $N = 50$ , indicating their limitations in figuring out shorter navigational paths in environments with a substantial number of agents.

**Omnidrones:** We report the training performance in Fig. 5 and the evaluation results in Tab. II. The experimental results show that MASP is superior to other competitors with a *Success Rate* of 100% in  $N = 5$  and 96% in  $N = 20$  in this complex 3-D environment. Except for MAGE-X, other RL baselines only have around 50% *Success Rate* in  $N = 5$ , indicating that they fail to directly solve the navigation problem in

Agents	Metrics	ORCA	RRT	Voronoi	MAPPO	DARL1N	MAGE-X	MASP
N = 5	Steps ↓	14.82(0.84)	7.66(1.89)	8.76(1.27)	8.62(1.38)	\	13.06(0.93)	<b>7.26(1.23)</b>
	SR ↑	0.88(0.01)	<b>1.00(0.00)</b>	<b>1.00(0.00)</b>	<b>1.00(0.00)</b>	0.78(0.02)	<b>1.00(0.00)</b>	<b>1.00(0.00)</b>
N = 20	Steps ↓	36.98(2.34)	34.74(3.31)	25.00(2.51)	\	\	\	<b>24.41(2.66)</b>
	SR ↑	0.95(0.02)	0.99(0.01)	<b>1.00(0.00)</b>	0.71(0.02)	0.62(0.03)	0.75(0.02)	<b>1.00(0.00)</b>
N = 50	Steps ↓	82.52(5.35)	79.20(4.30)	54.92(4.28)	\	\	\	<b>44.89(5.93)</b>
	SR ↑	0.96(0.01)	0.97(0.01)	<b>0.98(0.01)</b>	0.01(0.01)	0.49(0.02)	0.23(0.01)	<b>0.98(0.01)</b>

TABLE I: Performance of MASP, planning-based baselines and RL-based baselines with  $N = 5, 20, 50$  agents in MPE. The backslash in Steps denotes the agents can not reach the target 100% *Success Rate* in any episode.

Agents	Metrics	ORCA	RRT	Voronoi	MAPPO	DARL1N	MAGE-X	MASP
N = 5	Steps ↓	273.06(13.29)	144.30(14.51)	194.48(16.85)	\	\	231.26(19.32)	<b>138.35(13.57)</b>
	SR ↑	0.83(0.04)	0.96(0.01)	0.91(0.03)	0.50(0.09)	0.68(0.02)	0.99(0.01)	<b>1.00(0.00)</b>
N = 20	Steps ↓	489(13.01)	339.28(17.31)	460.32(14.48)	\	\	\	<b>315.31(14.52)</b>
	SR ↑	0.90(0.02)	0.97(0.01)	0.91(0.01)	0.15(0.03)	0.15(0.01)	0.14(0.03)	<b>0.97(0.01)</b>

TABLE II: Performance of MASP, planning-based baselines and RL-based baselines with  $N = 5, 20$  agents in OmniDrones. The backslash in Steps denotes the agents fail to reach 100% *Success Rate* in any episode.

Agents	Metrics	ORCA	RRT	Voronoi	MASP
10 ⇒ 20	Steps ↓	39.94(2.41)	32.82(3.49)	32.96(3.28)	<b>25.67(3.88)</b>
	SR ↑	0.95(0.01)	<b>1.00(0.00)</b>	0.99(0.01)	<b>1.00(0.00)</b>
40 ⇒ 50	Steps ↓	64.60(4.22)	64.62(4.93)	63.66(4.97)	<b>56.03(4.34)</b>
	SR ↑	<b>1.00(0.00)</b>	<b>1.00(0.00)</b>	<b>1.00(0.00)</b>	<b>1.00(0.00)</b>
20 ⇒ 10	Steps ↓	37.1(3.49)	26.64(3.23)	28.02(3.84)	<b>22.47(3.50)</b>
	SR ↑	0.91(0.01)	<b>1.00(0.00)</b>	<b>1.00(0.00)</b>	<b>1.00(0.00)</b>
50 ⇒ 40	Steps ↓	59.84(5.14)	48.44(4.20)	47.94(5.37)	<b>41.25(4.01)</b>
	SR ↑	<b>1.00(0.00)</b>	<b>1.00(0.00)</b>	<b>1.00(0.00)</b>	<b>1.00(0.00)</b>

TABLE III: Performance of MASP and planning-based baselines with a varying team size in MPE.

the complex search space. However, as the number of agents increases to 20, MAGE-X merely achieves a 15% *Success Rate*. This implies that the MLP-based goal assignment mechanism struggles to provide targets that are convenient for agents to reach in large and complex environments.

In contrast to RL baselines, almost all planning-based baselines achieve a *Success Rate* of over 90%, primarily owing to the greedy goal assignment algorithm without duplication. Therefore, we focus more on *Steps* to evaluate their performance. Among the planning-based competitors, RRT has the best performance with 7.06% more *Steps* compared to MASP in  $N = 20$ . This indicates that the tree structure in RRT, which omits the consideration of kinematic constraints, can better adapt to complex 3-D environments. ORCA and Voronoi struggle to find shorter navigational paths in the environment under high-dimensional spaces and intricate constraints.

2) *Varying Team Sizes within an Episode*: We further consider the setting where the team size varies within an episode. We use " $N_1 \Rightarrow N_2$ " to denote that each episode starts with  $N_1$  agents and the team size immediately switches to  $N_2$  after one-third of the total timesteps. Note that MASP

Agents	Metrics	ORCA	RRT	Voronoi	MASP
10 ⇒ 20	Steps ↓	\	\	\	<b>476.20(17.59)</b>
	SR ↑	0.63(0.01)	0.77(0.01)	0.79(0.01)	<b>0.91(0.01)</b>
20 ⇒ 10	Steps ↓	\	\	\	<b>426.73(18.50)</b>
	SR ↑	0.84(0.03)	0.89(0.04)	0.59(0.03)	<b>0.94(0.01)</b>

TABLE IV: Performance of MASP and planning-based baselines with a varying team size in OmniDrones. The backslash in Steps denotes the agents can not reach the target 100% *Success Rate* in any episode.

is trained on the scenes with a fixed team size, therefore the varying team size setting is a zero-shot generalization challenge for MASP. We use the MASP model previously trained with  $N = \max(N_1, N_2)$ . Besides, the RL baselines lack generalization capabilities in either network architecture or final performance, thus we only compare MASP with planning-based methods.

**MPE**: Tab. III summarizes the zero-shot generalization performance in MPE. In cases where the team size increases, MASP produces substantially better performances. In particular in  $40 \Rightarrow 50$ , MASP achieves at least 11.99% fewer *Steps* than other methods, which suggests that MASP has the capability to adaptively adjust its strategy.

Regarding the cases where the team size decreases, the difference between the methods becomes more pronounced. Specifically, MASP consumes 13.95% fewer *Steps* than Voronoi in  $40 \Rightarrow 50$ . We remark that decreasing the team size is particularly challenging, as the absence of certain agents may result in a situation where some targets remain unassigned. Consequently, the team should continuously update its plan and adopt markedly different goal assignment strategies when previously assigned goals are achieved at each global step.



**OmniDrones:** Tab. IV presents the evaluation results about the zero-shot generalization in OmniDrones. In scenarios where the team size increases, some targets may be occupied by multiple agents that are so close to each other that a crash occurs. Therefore, all baselines fail to reach a 100% *Success Rate* in any episode due to their poor coordination strategies. In contrast, MASP performs best with an average *Success Rate* of 91%.

In scenarios where the team size decreases, the planning-based baselines still fail to reach a 100% *Success Rate* in any episode. This challenge stems from the fact that the absence of certain agents requires the remaining agents to dynamically adjust their plans to reach goals that exceed the total number of the remaining agents. This is particularly difficult in such a complex 3-D environment. Conversely, MASP maintains an average *Success Rate* of 94% due to its flexible and adaptive strategy.

#### F. Ablation Studies

To illustrate the effectiveness of each component of MASP, we consider 3 variants of our method in MPE with 20 agents:

- **MASP w. RG:** We substitute MGM with random sampling without replacement to assign each agent a random target goal.
- **MGM w.o. Graph:** We consider the MLP layer as an alternative to MGM for assigning the target goal to each agent at each global step. The MLP layer takes in the concatenation of the position information of all the agents and goals for agent  $k$ , where the position information of agent  $k$  is concatenated first.
- **CAE w.o. Graph:** We consider the MLP layer as a substitute for CAE to capture the correlation between agents and goals. The input to the MLP layer for agent  $k$  comprises the position information of all the agents and the assigned goal for agent  $k$ .

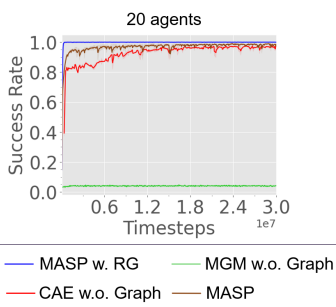


Fig. 6: Ablation study on MASP in MPE with 20 agents.

perceive the intricate correlations between agents and target goals based on the given information. *MASP w. RG* always assigns different goals to agents, enabling it to attain a 100% *Success Rate*. However, due to the lack of an appropriate goal assignment, it requires 32.02% more *Steps* to achieve the target *Success Rate*. *CAE w.o. Graph* is slightly inferior to MASP with slower training convergence and 13.59% more *Steps* in the evaluation. This indicates that in contrast

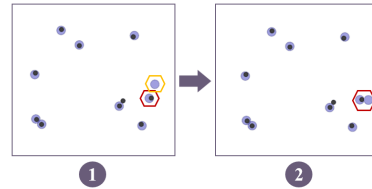
To demonstrate the performance of MASP and its variants, we report the training curves in Fig. 6 and the evaluation results in Tab. V. MASP outperforms its counterparts with a 100% *Success Rate* and the fewest *Steps*. *MGM w.o. Graph* degrades the most, suggesting that without the graph matching, MGM struggles to

Agents	Metrics	MASP w. RG	MGM-MLP	CAE-MLP	MASP
N =20	Steps ↓	35.91(2.73)	\	28.25(3.21)	<b>24.41(2.66)</b>
	SR ↑	<b>1.00(0.00)</b>	0.04(0.01)	<b>1.00(0.00)</b>	<b>1.00(0.00)</b>

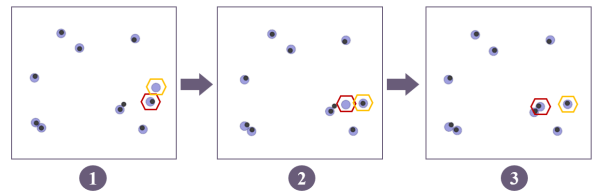
TABLE V: Performance of MASP and RL variants with  $N = 20$  agents in MPE. The backslash in Steps denotes the agents can not reach the target 100% success rate in any episode.

to the MLP layer, the GNN in CAE better captures the relationships between agents and assigned goals.

#### G. Learned Strategies



(a) Learned strategy of DARL1N



(b) Learned strategy of MASP

Fig. 7: The comparison in learned strategies of DARL1N and MASP in MPE.

Under the decentralized decision-making paradigm, agents need to make decisions independently, which is challenging to achieve team objectives. As depicted in Fig. 7, we compare the learned strategies of DARL1N and MASP to showcase that MASP addresses this issue with high cooperation. To be specific, agents that make independent decisions potentially lead to situations where the agent in the red pentagon and the agent in the yellow pentagon select the same goal to reach. In Fig. 7(a), these two DARL1N agents fail to adjust their strategies promptly and finally stay at the same target. On the contrary, as shown in Fig. 7(b), when the red MASP agent notices that the yellow MASP agent moves toward the same goal, it changes its strategy and redirects to an unexplored goal at the next global decision-making step. Therefore, MASP agents are able to occupy different goals separately, resulting in a 100% *Success Rate* with high cooperation.

## VI. CONCLUSION AND FUTURE WORK

We propose a decentralized, goal-conditioned hierarchical planner, *Multi-Agent Scalable GNN-based Planner*, to improve data efficiency and cooperation in navigation tasks with a substantial number of agents. In MASP, the Multi-Goal Matcher leverages graph matching to allocate target goals to agents at each global step, and the Coordinated Action Executor utilizes GNN to capture team representation with strong goal guidance. We further divide the agents into

several groups with a fixed trained number of agents to enhance the generalization capability in scenarios with unseen agent count. Thorough experiments demonstrate that MASP achieves higher sample efficiency and better performance than classical planning-based baselines and RL competitors in MPE and Omnidrones with large and varying numbers of agents. Currently, MASP mainly focuses on multi-agent navigation tasks, and we hope to extend MASP to other multi-agent applications in the future.

## REFERENCES

- [1] G. Bresson, Z. Alsayed, L. Yu, and S. Glaser, "Simultaneous localization and mapping: A survey of current trends in autonomous driving," *IEEE Transactions on Intelligent Vehicles*, vol. 2, no. 3, pp. 194–220, 2017.
- [2] S. Grigorescu, B. Trasnea, T. Cocias, and G. Macesanu, "A survey of deep learning techniques for autonomous driving," *Journal of Field Robotics*, vol. 37, no. 3, pp. 362–386, 2020.
- [3] S. Liu and L. Hu, "Application of beidou navigation satellite system in logistics and transportation," in *Logistics: The Emerging Frontiers of Transportation and Development in China*, 2009, pp. 1789–1794.
- [4] K. Gao, J. Xin, H. Cheng, D. Liu, and J. Li, "Multi-mobile robot autonomous navigation system for intelligent logistics," in *2018 Chinese Automation Congress (CAC)*. IEEE, 2018, pp. 2603–2609.
- [5] A. Kleiner, J. Prediger, and B. Nebel, "Rfid technology-based exploration and slam for search and rescue," in *2006 IEEE/RSJ International Conference on Intelligent Robots and Systems*. IEEE, 2006, pp. 4054–4059.
- [6] D. Calisi, A. Farinelli, L. Iocchi, and D. Nardi, "Autonomous navigation and exploration in a rescue environment," in *IEEE International Safety, Security and Rescue Robotics, Workshop, 2005*. IEEE, 2005, pp. 54–59.
- [7] W. Burgard, M. Moors, C. Stachniss, and F. E. Schneider, "Coordinated multi-robot exploration," *IEEE Transactions on robotics*, vol. 21, no. 3, pp. 376–386, 2005.
- [8] H. Umari and S. Mukhopadhyay, "Autonomous robotic exploration based on multiple rapidly-exploring randomized trees," in *2017 IEEE/RSJ International Conference on Intelligent Robots and Systems (IROS)*, 2017, pp. 1396–1402.
- [9] C. Yu, X. Yang, J. Gao, H. Yang, Y. Wang, and Y. Wu, "Learning efficient multi-agent cooperative visual exploration," in *European Conference on Computer Vision*. Springer, 2022, pp. 497–515.
- [10] X. Yang, S. Huang, Y. Sun, Y. Yang, C. Yu, W.-W. Tu, H. Yang, and Y. Wang, "Learning graph-enhanced commander-executor for multi-agent navigation," in *Proceedings of the 2023 International Conference on Autonomous Agents and Multiagent Systems*, 2023, pp. 1652–1660.
- [11] L. Xia, C. Yu, and Z. Wu, "Inference-based hierarchical reinforcement learning for cooperative multi-agent navigation," in *2021 IEEE 33rd International Conference on Tools with Artificial Intelligence (ICTAI)*. IEEE, 2021, pp. 57–64.
- [12] C. Yu, A. Velu, E. Vinitsky, Y. Wang, A. Bayen, and Y. Wu, "The surprising effectiveness of ppo in cooperative, multi-agent games," *arXiv preprint arXiv:2103.01955*, 2021.
- [13] M. Wen, J. G. Kuba, R. Lin, W. Zhang, Y. Wen, J. Wang, and Y. Yang, "Multi-agent reinforcement learning is a sequence modeling problem," *arXiv preprint arXiv:2205.14953*, 2022.
- [14] C. Wakilpoor, P. J. Martin, C. Rebhuhn, and A. Vu, "Heterogeneous multi-agent reinforcement learning for unknown environment mapping," *arXiv preprint arXiv:2010.02663*, 2020.
- [15] X. Liu, D. Guo, H. Liu, and F. Sun, "Multi-agent embodied visual semantic navigation with scene prior knowledge," *arXiv preprint arXiv:2109.09531*, 2021.
- [16] R. Lowe, Y. I. Wu, A. Tamar, J. Harb, O. Pieter Abbeel, and I. Mordatch, "Multi-agent actor-critic for mixed cooperative-competitive environments," *Advances in neural information processing systems*, vol. 30, 2017.
- [17] B. Xu, F. Gao, C. Yu, R. Zhang, Y. Wu, and Y. Wang, "Omnidrones: An efficient and flexible platform for reinforcement learning in drone control," *arXiv preprint arXiv:2309.12825*, 2023.
- [18] S. Zhang, Y. Li, and Q. Dong, "Autonomous navigation of uav in multi-obstacle environments based on a deep reinforcement learning approach," *Applied Soft Computing*, vol. 115, p. 108194, 2022.
- [19] M. Martini, S. Cerrato, F. Salvetti, S. Angarano, and M. Chiaberge, "Position-agnostic autonomous navigation in vineyards with deep reinforcement learning," in *2022 IEEE 18th International Conference on Automation Science and Engineering (CASE)*. IEEE, 2022, pp. 477–484.
- [20] X. Yang, C. Yu, J. Gao, Y. Wang, and H. Yang, "Save: Spatial-attention visual exploration," in *2022 IEEE International Conference on Image Processing (ICIP)*. IEEE, 2022, pp. 1356–1360.
- [21] R. Han, S. Chen, S. Wang, Z. Zhang, R. Gao, Q. Hao, and J. Pan, "Reinforcement learned distributed multi-robot navigation with reciprocal velocity obstacle shaped rewards," *IEEE Robotics and Automation Letters*, vol. 7, no. 3, pp. 5896–5903, 2022.
- [22] B. Wang, J. Xie, and N. Atanasov, "DarlIn: Distributed multi-agent reinforcement learning with one-hop neighbors," in *2022 IEEE/RSJ International Conference on Intelligent Robots and Systems (IROS)*. IEEE, 2022, pp. 9003–9010.
- [23] D. Hafner, K.-H. Lee, I. Fischer, and P. Abbeel, "Deep hierarchical planning from pixels," *Advances in Neural Information Processing Systems*, vol. 35, pp. 26 091–26 104, 2022.
- [24] Y. Takubo, H. Chen, and K. Ho, "Hierarchical reinforcement learning framework for stochastic spaceflight campaign design," *Journal of Spacecraft and rockets*, vol. 59, no. 2, pp. 421–433, 2022.
- [25] S. Nasiriany, H. Liu, and Y. Zhu, "Augmenting reinforcement learning with behavior primitives for diverse manipulation tasks," in *2022 International Conference on Robotics and Automation (ICRA)*. IEEE, 2022, pp. 7477–7484.
- [26] R. Wang, R. Yu, B. An, and Z. Rabinovich, "I2hrl: Interactive influence-based hierarchical reinforcement learning," in *Proceedings of the Twenty-Ninth International Conference on International Joint Conferences on Artificial Intelligence*, 2021, pp. 3131–3138.
- [27] A. P. Pope, J. S. Ide, D. Mićović, H. Diaz, D. Rosenbluth, L. Ritholtz, J. C. Twedt, T. T. Walker, K. Alcedo, and D. Javorek, "Hierarchical reinforcement learning for air-to-air combat," in *2021 international conference on unmanned aircraft systems (ICUAS)*. IEEE, 2021, pp. 275–284.
- [28] F. Scarselli, M. Gori, A. C. Tsoi, M. Hagenbuchner, and G. Monfardini, "The graph neural network model," *IEEE transactions on neural networks*, vol. 20, no. 1, pp. 61–80, 2008.
- [29] Y. Liu, K. Zeng, H. Wang, X. Song, and B. Zhou, "Content matters: A gnn-based model combined with text semantics for social network cascade prediction," in *Pacific-Asia Conference on Knowledge Discovery and Data Mining*. Springer, 2021, pp. 728–740.
- [30] S. Zhang, Y. Liu, and L. Xie, "Molecular mechanics-driven graph neural network with multiplex graph for molecular structures," *arXiv preprint arXiv:2011.07457*, 2020.
- [31] Y. Liu, W. Wang, Y. Hu, J. Hao, X. Chen, and Y. Gao, "Multi-agent game abstraction via graph attention neural network," in *Proceedings of the AAAI Conference on Artificial Intelligence*, vol. 34, no. 05, 2020, pp. 7211–7218.
- [32] X. Jia, L. Sun, H. Zhao, M. Tomizuka, and W. Zhan, "Multi-agent trajectory prediction by combining egocentric and allocentric views," in *Conference on Robot Learning*. PMLR, 2022, pp. 1434–1443.
- [33] J. Schulman, F. Wolski, P. Dhariwal, A. Radford, and O. Klimov, "Proximal policy optimization algorithms," *arXiv preprint arXiv:1707.06347*, 2017.
- [34] M. Turpin, K. Mohta, N. Michael, and V. Kumar, "Goal assignment and trajectory planning for large teams of interchangeable robots," *Autonomous Robots*, vol. 37, no. 4, pp. 401–415, 2014.
- [35] B. P. Gerkey and M. J. Mataric, "A formal analysis and taxonomy of task allocation in multi-robot systems," *The International journal of robotics research*, vol. 23, no. 9, pp. 939–954, 2004.
- [36] R. Burkard, M. Dell'Amico, and S. Martello, *Assignment problems: revised reprint*. SIAM, 2012.
- [37] A. Vaswani, N. Shazeer, N. Parmar, J. Uszkoreit, L. Jones, A. N. Gomez, E. Kaiser, and I. Polosukhin, "Attention is all you need," *Advances in neural information processing systems*, vol. 30, 2017.
- [38] K. Guo, D. Wang, T. Fan, and J. Pan, "Vr-orca: Variable responsibility optimal reciprocal collision avoidance," *IEEE Robotics and Automation Letters*, vol. 6, no. 3, pp. 4520–4527, 2021.
- [39] J. Hu, H. Niu, J. Carrasco, B. Lennox, and F. Arvin, "Voronoi-based multi-robot autonomous exploration in unknown environments via deep reinforcement learning," *IEEE Transactions on Vehicular Technology*, vol. 69, no. 12, pp. 14 413–14 423, 2020.